

## Transient enhanced diffusion after laser thermal processing of ion implanted silicon

Kevin S. Jones,<sup>a)</sup> Heather Banisaukas, and Josh Glassberg

*Department of Materials Science and Engineering, SWAMP Center, University of Florida, Gainesville, Florida 32611*

Ebrahim Andideh

*Intel Corporation, Portland, Oregon 97124*

Craig Jasper and Allen Hoover

*Motorola, Mesa, Arizona 85202*

Aditya Agarwal

*Eaton Corporation, Beverly, Massachusetts 01915*

Mike Rendon

*Motorola, Austin, Texas 78741*

(Received 9 August 1999; accepted for publication 11 October 1999)

The effect of laser thermal processing (LTP) on implantation-induced defect evolution and transient enhanced diffusion (TED) of boron was investigated. A 270-Å-thick amorphous layer formed by 10 keV Si<sup>+</sup> implantation was melted and regrown using a 20 ns ultraviolet laser pulse. Transmission electron microscopy revealed that recrystallization of the amorphous layer following LTP results in a high concentration of stacking faults and microtwins in the regrown region. Also, the end-of-range loop evolution during subsequent 750 °C furnace annealing, is different in a LTP sample compared to a control sample. Secondary ion mass spectroscopy of a boron marker layer 6000 Å below the surface showed that LTP alone produced no enhanced diffusion. However, during subsequent furnace annealing, the boron layer in the LTP sample experienced just as much TED as in the control sample which was only implanted and furnace annealed. These results imply that laser melting and recrystallization of an implantation-induced amorphous layer does not measurably reduce the excess interstitials released from the end-of-range implant damage. © 1999 American Institute of Physics. [S0003-6951(99)00149-7]

Continued scaling of the transistor to sub-100 nm dimensions requires the formation of ultrashallow highly doped abrupt junctions for contact formation. A box-shaped, high dopant concentration profile could ideally meet such a requirement.<sup>1</sup> Ion implantation and conventional rapid thermal annealing inevitably lead to less than ideal Gaussian or exponential dopant profile. Also, the interaction between implantation induced point defects and dopant atoms during annealing can considerably broaden the profile shape through transient enhanced diffusion (TED). One proposed method for circumventing some of these problems is the use of laser annealing.<sup>2</sup> Various approaches proposed include: melting and regrowing crystalline silicon in the presence of a dopant (the PGILD process) or preamorphization of the surface by implantation followed by a dopant implant into the amorphous material and finally laser melting only the amorphous material [also called laser thermal processing (LTP)].<sup>2-4</sup> The advantage of the second method is that lower temperatures can be used because amorphous Si melts at a temperature 300 °C lower than crystalline Si. This is important because it allows thickness of the melted region to be controlled by the preamorphization.

One question that remains is does LTP have an advantage in the transient enhanced diffusion reduced from the

implant. It is well known that after implantation induced amorphization of Si, there exists a highly damaged region in the crystalline material just beyond the amorphous/crystalline interface.<sup>5</sup> This layer, referred to as the end-of-range (EOR) damage region, is known to contain a large supersaturation of interstitials. During annealing these interstitials are released and flow both toward the surface and into the bulk, resulting in TED of the common dopants (e.g., B, As, P).<sup>6</sup> This TED has the undesirable effect of greatly enhancing the junction depth and resulting in reverse short channel effects.<sup>7</sup> Here we investigate whether laser melting and recrystallization of the amorphous layer during LTP reduces the interstitial flux originating from the end-of-range damage region.

A single boron-doped marker layer, with a peak concentration of  $3 \times 10^{18} \text{ cm}^{-3}$  and a full width at half max value of 150 Å, followed by 5800 Å of undoped Si was epitaxially grown by chemical vapor deposition (CVD) on a 200 mm silicon wafer. The CVD was done in a commercial Si epitaxial system using a SiCl<sub>2</sub>H<sub>2</sub> source at 800 °C. A 350 Å oxide capping layer was deposited *in situ* at 380 °C after the CVD growth. Boron diffusion was measured by secondary ion mass spectrometry (SIMS) using 3 keV O<sub>2</sub><sup>+</sup> primary ion bombardment and positive secondary ion detection. Plan-view and cross-sectional transmission electron microscopy (TEM) samples were prepared by standard procedures.

<sup>a)</sup>Electronic mail: kjones@eng.ufl.edu

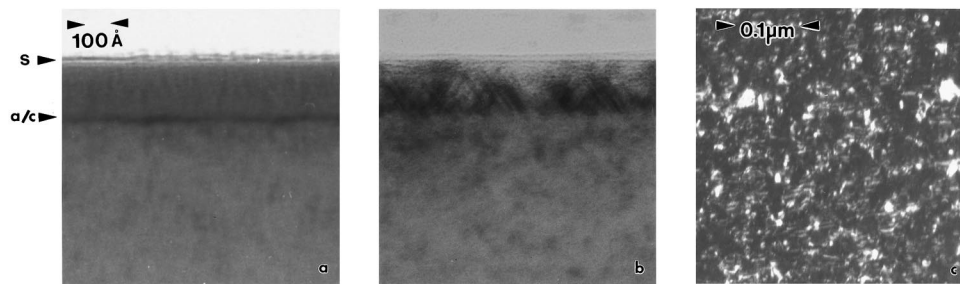


FIG. 1. Cross-sectional TEM micrographs for the (a) as-implanted sample,  $10 \text{ keV Si}^+ 1 \times 10^{15} \text{ cm}^{-2}$  (b) after laser thermal processing (c) plan-view TEM micrograph of the laser thermal processed sample. Note the high density of stacking faults and microtwins present after LTP processing.

The quality of the CVD-grown epitaxial Si was characterized by annealing a marker layer sample at  $750^\circ\text{C}$  for 6 h. Comparison of the as-grown and diffused B profiles yielded a value for the B diffusivity within a factor of two of the predicted equilibrium diffusivity.<sup>8</sup>

Prior to laser thermal processing, the oxide cap on the Si was stripped using a buffered-oxide etch and the sample surface was amorphized using a  $10 \text{ keV}, 1 \times 10^{15} \text{ cm}^{-2} \text{ Si}^+$  implant. Figure 1(a) shows by cross-sectional TEM that this implant resulted in an amorphous layer approximately  $270 \text{ \AA}$  deep. Following implantation, the amorphous layer was melted and recrystallized by LTP. This involved exposure of a  $2 \text{ mm} \times 8 \text{ mm}$  region, to a  $308 \text{ nm}$  ultraviolet (UV) laser pulse at a power of  $0.70 \text{ J/cm}^2$ . The pulse duration was approximately 20 ns. These conditions were chosen to confine the melt to the amorphous layer. Figures 1(b) and 1(c) show cross-sectional and a plan-view images, respectively, of the regrown layer after only LTP. A high density of stacking faults and microtwins can be seen after LTP. The depth of the defected layer corresponds to the thickness of the amorphous layer. It is presumed that the crystalline Si underneath the amorphous layer was not melted during rapid thermal processing (RTP), however, this cannot be confirmed.

Figures 2(a) and 2(b) show the plan-view TEM results

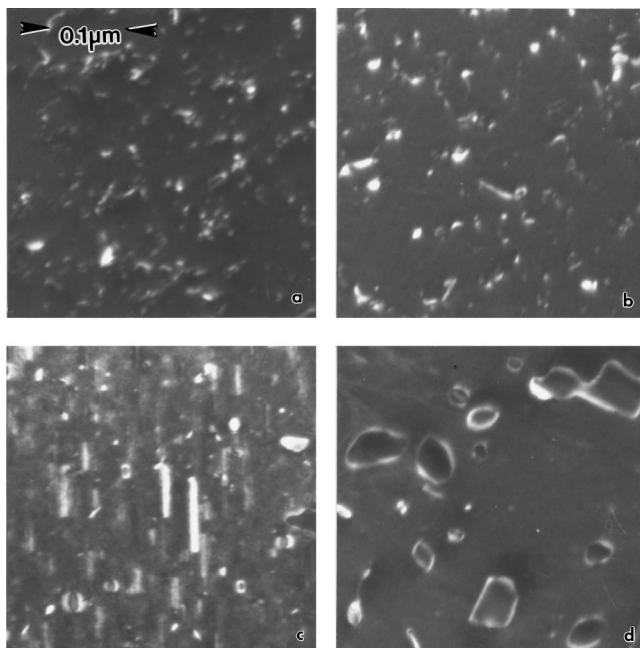


FIG. 2. Plan-view  $g_{220}$  TEM micrographs showing the effects of furnace annealing on implanted samples with (a) LTP processing after  $750^\circ\text{C}$  15 min annealing, (b) LTP processing after  $750^\circ\text{C}$  360 min annealing, (c) no LTP processing after  $750^\circ\text{C}$  15 min annealing, (d) no LTP processing after  $750^\circ\text{C}$  360 min annealing.

after LTP and furnace annealing at  $750^\circ\text{C}$  for times of 15 min and 6 h, respectively. A comparison of Fig. 2(a) with Fig. 1 shows that annealing for 15 min significantly reduces the concentration of microtwins and stacking faults. Further annealing for between 15 min and 6 h does not have a significant effect on the defect density. Figures 2(c) and 2(d) show plan-view TEM images of a control sample which received the same implant and furnace anneals but no LTP step. Figure 2(c) shows that  $\{311\}$  defects including zigzag defects<sup>9</sup> normally associated with such low energy implants have formed in addition to small dislocation loops. Cross-sectional TEM confirmed these defects are located in the EOR region as expected. Figure 2(d) shows that, upon further annealing, the  $\{311\}$  defects dissolve and/or unfault and only dislocation loops remain. Cross-sectional TEM showed these loops range in depth from 100 to  $300 \text{ \AA}$ . From a comparison of Figs. 2(a) and 2(c) the LTP process appears to prevent the nucleation of  $\{311\}$  defects.

The SIMS profile of the boron-doping marker layer exhibited no broadening after ion implantation and laser thermal processing relative to the as-grown marker layer. Figure 3 compares the diffused B profiles in three different samples

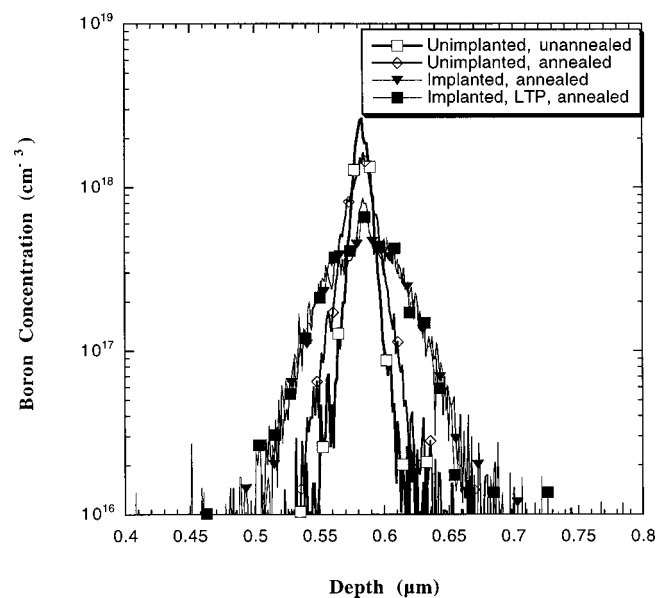


FIG. 3. SIMS of the buried boron marker layer for three different samples after furnace annealing at  $750^\circ\text{C}$  for 6 h. The as-grown sample profile is shown (open squares). One sample received no implantation and no laser thermal processing (LTP) step but was annealed (open diamonds) and showed only normal boron diffusion. The third sample received an implantation step but no LTP step (triangles) prior to furnace annealing and showed an enhancement indicative of TED from the end of range damage (upside down triangles). The fourth sample received both the ion implantation (II) and LTP steps prior to furnace annealing and yet still showed enhanced diffusion indicative of TED (solid squares).

after annealing at 750 °C for 6 h. One control sample was unimplanted with no laser annealing and had received only the furnace anneal. The diffusion observed relative to the unannealed spike was within a factor of two of the predicted inert diffusivity as mentioned previously. A second control sample received the implant and the furnace anneal but no laser annealing. The third sample received both the implant and the LTP step prior to furnace annealing. Both samples, which received the amorphizing implant, showed a significant enhancement relative to the unimplanted sample. The time averaged diffusivity enhancement factor  $\langle D_B \rangle / D_B^*$  of 16 was estimated using the process simulator FLOOPS<sup>10</sup> as described elsewhere.<sup>11</sup> Here  $D_B$  is the observed diffusivity and  $D_B^*$  the equilibrium diffusivity. This value of time averaged enhancement is less than what is normally observed for TED but the annealing time was very long (6 h) and the amorphous layer was very shallow. Both factors would contribute to a smaller  $\langle D_B \rangle / D_B^*$ .

Figure 3 shows that the boron diffusion associated with samples that had received both the implant and the LTP process prior to annealing is the same as that in the second control, which received the implant but no LTP. This implies that the same interstitial flux is released from the implanted region regardless of whether the sample receives a LTP anneal or not. The LTP process therefore melts and recrystallizes the amorphous layer without significantly reducing the concentration of interstitials released into the crystal. The lack of 311 defects in the TEM micrographs of Fig. 2 implies that the excess interstitials in the end-of-range region were either redistributed by the LTP step, such that the concentration supersaturation is below that needed for extended defect nucleation or there was an alternative sink. The interstitial dose in the end-of-range for the control sample is above  $1 \times 10^{14} \text{ cm}^2$  (estimated from quantitative TEM of the control sample after 15 min annealing) and the threshold interstitial dose for {311} formation is around or below  $1 \times 10^{13} \text{ cm}^2$ .<sup>12</sup> Thus a dilution of the interstitials by a factor of at least 10 would be needed to prevent {311} formation. This would require a significant amount of diffusion during the LTP process. Shallow junctions formed by this step show no signs of any measurable boron motion into the crystal after LTP processing (one of the reasons for using this method to produce shallow junctions). Thus it is unlikely the lack of defect formation in the EOR is the result of massive interstitial diffusion during LTP. The second alternative is that there is a competing sink for the interstitials. Given the high concen-

tration of stacking faults and microtwins in the regrown region, it is possible that these extended defects act as a sink for the excess interstitials in the EOR. These defects do show some dissolution upon furnace annealing and thus these may act as a source of interstitials for TED. Further experimentation is needed to confirm this suggestion. Whatever the explanation, it is curious that the total TED is so similar yet the extended defect evolution is dramatically different.

In conclusion, it is clear that there are many factors that are not understood after laser thermal processing. It has been shown that laser melting and recrystallization of an implantation induced amorphous layer eliminates the formation of end of range dislocation loops. However the process can introduce very high concentrations of alternative regrowth defects. Despite the change in morphology, LTP processing does not measurably reduce the transient enhanced diffusion observed in using a buried marker layer. It is critical for process integration that the location and evolution of these excess interstitials be determined. Additional studies into the effects of changing the laser processing and annealing conditions on TED are in progress.

The authors would like to acknowledge the assistance of Somit Talwar at Verdant Technologies for performing the laser thermal processing. Also the authors would like to thank Erica Heitman for her assistance with the TEM sample preparation and ESB for additional assistance. This work was supported by Grant No. MBP-D003 from SEMATECH.

- <sup>1</sup>Y. Taur, C. H. Wann, and D. J. Frank, Tech. Dig. Int. Electron Devices Meet. **98**, 789 (1998).
- <sup>2</sup>E. C. Jones and E. Ishida, Mater. Sci. Eng., R. **24**, 1 (1998).
- <sup>3</sup>K.-J. Kramer, S. Talwar, I. T. Lewis, J. E. Davison, K. A. Williams, K. A. Benton, and K. H. Weiner, Appl. Phys. Lett. **68**, 2320 (1996).
- <sup>4</sup>P. G. Carey, T. W. Sigmon, R. L. Press, and T. S. Fahlen, IEEE Electron Device Lett. **6**, 291 (1985).
- <sup>5</sup>K. S. Jones, V. Krishnamoorthy, L. H. Zhang, M. Law, D. S. Simons, P. H. Chi, L. Rubin, and R. G. Elliman, Appl. Phys. Lett. **68**, 2672 (1996).
- <sup>6</sup>K. S. Jones, R. G. Elliman, M. M. Petracic, and P. Kringhoj, Appl. Phys. Lett. **68**, 3111 (1996).
- <sup>7</sup>C. S. Rafferty, H.-H. Vuong, S. A. Eshraghi, M. D. Giles, M. R. Pinto, and S. J. Hillenius, Tech. Dig. Int. Electron Devices Meet. **93**, 311 (1993).
- <sup>8</sup>R. B. Fair, in *Impurity Doping Processes in Silicon*, edited by F. F. Y. Wang (North Holland, New York, 1981), p. 968.
- <sup>9</sup>A. Agarwal, T. Haynes, D. Eaglesham, H.-J. Gossman, D. Jacobson, J. Poate, and Y. Erokhin, Appl. Phys. Lett. **70**, 3332 (1997).
- <sup>10</sup>M. E. Law and S. M. Cea, Comput. Mater. Sci. **12**, 289 (1998).
- <sup>11</sup>H.-J. Gossmann, C. S. Rafferty, H. S. Luftman, F. C. Unterwald, and T. Boone, Appl. Phys. Lett. **63**, 639 (1993).
- <sup>12</sup>D. J. Eaglesham, P. A. Stolk, H.-J. Gossmann, and J. M. Poate, Appl. Phys. Lett. **65**, 2305 (1994).